IOP Publishing Physical Biology
Phys. Biol. 11 (2014) 044001 (6pp) doi:10.1088/1478-3975/11/4/044001

Note

Electrostatic effect of H1-histone protein binding on nucleosome repeat length

Andrey G Cherstvy[1] **and Vladimir B Teif**[2]

[1] Institute for Physics and Astronomy, University of Potsdam, 14476 Potsdam-Golm, Germany
[2] Deutsches Krebsforschungszentrum (DKFZ) and BioQuant, 69120 Heidelberg, Germany

E-mail: a.cherstvy@gmail.com

Received 1 April 2014, revised 30 June 2014
Accepted for publication 3 July 2014
Published 31 July 2014

Abstract

Within a simple biophysical model we describe the effect of electrostatic binding of H1 histone proteins on the nucleosome repeat length in chromatin. The length of wrapped DNA optimizes its binding energy to the histone core and the elastic energy penalty of DNA wrapping. The magnitude of the effect predicted from our model is in agreement with the systematic experimental data on the linear variation of nucleosome repeat lengths with H1/nucleosome ratio (Woodcock C L *et al* 2006 *Chromos. Res.* **14** 17–25). We compare our model to the data for different cell types and organisms, with a widely varying ratio of bound H1 histones per nucleosome. We underline the importance of this non-specific histone-DNA charge-balance mechanism in regulating the positioning of nucleosomes and the degree of compaction of chromatin fibers in eukaryotic cells.

Keywords: electrostatics, DNA, nucleosome

(Some figures may appear in colour only in the online journal)

Introduction

Eukaryotic DNA is packed inside tiny nuclei by highly-ordered wrapping of 147 base pairs (bp) of DNA around the core histone octamer to form the nucleosome. Apart from core histones, other architectural chromatin proteins including linker histones contribute to DNA compaction. The nucleosome core particle (NCP) is the elementary unit of DNA organization in eukaryotes [1, 2]. Positioning of NCPs on genomic DNAs [3, 4], the implications of competitive histone binding to DNA with a myriad of transcription factors [5–9], and the accessibility of genetic information upon transcription [10] are the questions of paramount importance for molecular and cell biophysics.

The atomistic structure of isolated NCPs is known from x-ray crystal data and it can be implemented in molecular dynamics simulations. On the other hand, many tasks require considering dozens and hundreds of nucleosomes, which is not achievable at the atomic resolution on realistic time-scales. At the scales when atomistic details become negligible, integrative parameters become more important, such as the average distance between neighboring nucleosomes, the so called nucleosome repeat length (NRL). The latter varies from 154 bp in fission yeast to 240 bp in some of the cell types in higher eukaryotes [1].

To address the problem of NRL calculation, it is sometimes enough to introduce a toy model for individual NCPs (figure 1(A)) and use simplified mathematical constructs on higher levels of DNA organization [8]. One class of such models is based on the assumption that linker histones H1 prefer to bind between the nucleosomes. This allows the studying of nucleosome/H1 competition in the spirit of classical 1D DNA lattice models with excluded-volume interactions [11, 12] (figure 1(B)). At another extreme is the assumption that H1 and other NCP-binding proteins bind to the nucleosome core, leaving the linker DNA free. In the latter case, electrostatics (ES) is likely to dominate. To a first approximation, one can assume that nucleosome-binding proteins 'dissolve' in the core increasing its positive charge, which is to be compensated by the wrapped oppositely charged DNA (figure 1(C)).

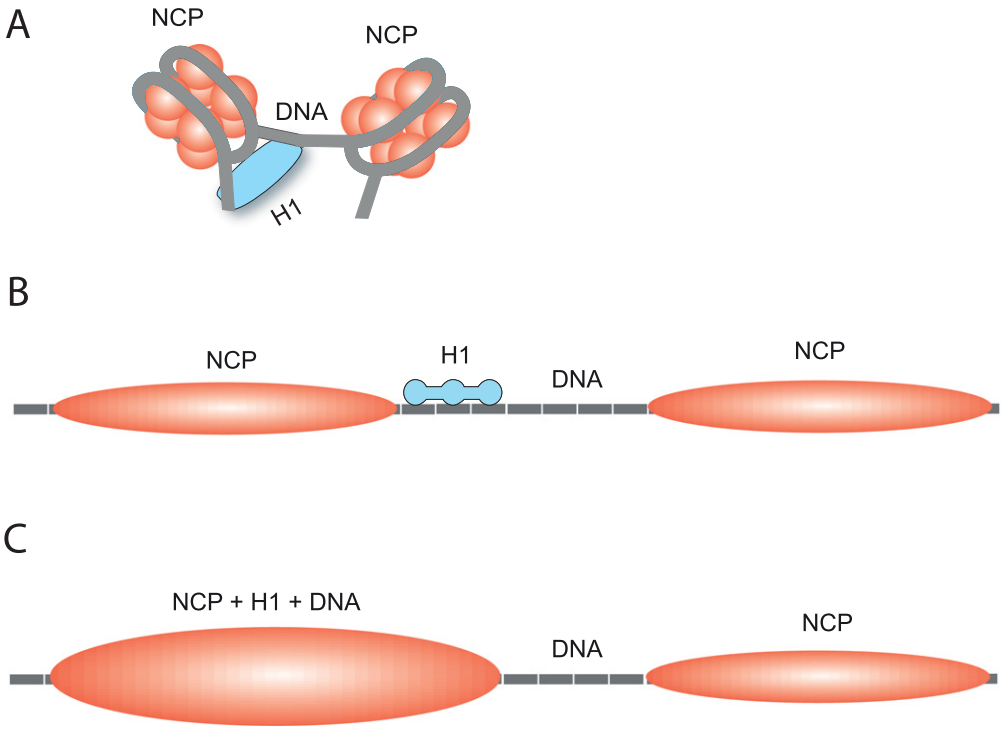

Figure 1. Toy models for NCP complexes with linker histones. (A) 147 bps of DNA are wrapped around the histone octamer, while the linker histone H1 binds close to the nucleosome entry/exit, physically interacting with both DNA and core histones and likely softening the linker DNA [1]. (B) Large-scale 1D lattice models can be constructed assuming that H1 binds mostly to the DNA between nucleosomes, thus increasing NRL by effectively 'repelling' neighbouring NCPs. (C) At another extreme, bound H1 effectively becomes a part of NCP, increasing the charge that needs to be neutralized by a longer DNA stretch. This leads to a corresponding NRL increase and more DNA bps are 'integrated' in the nucleosome.

Here we use such a toy model to rationalize the NRL variation with the amount of NCP-bound linker H1 histones, as measured experimentally in great detail by Woodcock *et al* [13], Blanck and Becker [14], Fan *et al* [15, 16], and Bates and Thomas [17]. These publications mention that NRL values increase with increasing concentrations of K^+, Mg^{2+}, polyamines, and particularly H1 histone family proteins, supporting the significance of the electrostatic balance [18]. Due to space limitations, the reader is referred to the original papers cited in [13] and more recently [19] (see also the conclusions section) to gain more biological insights on the vital role of linker histones in formation and stability of chromatin fibers, the spatial arrangements of nucleosomes, transcriptional regulation of the chromatin (e.g. transcriptionally active chromatin is often depleted in H1), and the effect of H1 histones on NRL in different cell types and organisms. These sets of data offer unambiguous evidence of the importance of non-specific ES effects in positioning of NCPs on genomic DNA, likely interfering with or accompanying the widely-recognized sequence-specific affinity code for the arrangement of NCPs on DNA [3, 20].

The model of ES-motivated DNA wrapping

We present a physical-chemical model of ES DNA binding to the histone core of an isolated NCP accounting for different amounts of the linker H1 histones bound per NCP. Our model implements ES attraction of a fragment of negatively charged DNA to strongly positively charged histones. The bare charge of the DNA is due to the helically located phosphate groups, amounting to the net charge density of two elementary charges e_0 per one DNA bp, or $h = 3.4$ Å along the DNA axis. The histone core charges stems mainly from the basic Arg and Lys protein residues [21]. A number of theoretical and computational models of DNA wrapping in the NCP have been proposed in recent years [22–27]. However, the description of experimental data overviewed in [13], vital for rationalizing the properties of higher-order DNA compaction in chromatin, remained without proper theoretical attention. Addressing this issue is the main purpose of the current study.

The length of DNA bound in NCP is conserved to 146–147 bp among various cell types and organisms. The NRL variation takes place not because DNA fragments of different lengths get wrapped around the core histones, but rather because of different lengths of a free, unbound DNA. A varying length of DNA immobilized by the linker H1/H5 histones and severe geometrical restrictions [28] imposed on packing of nucleosomes in compact tightly-wound 30 nm chromatin fibers [29, 30] are considered in our separate publication [11]. In the current approach, the length of the histone-bound DNA *is* responsible for NRL variations with the amount of NCP-bound H1 proteins.

We treat the histone core octamer here as a uniformly positively charged sphere of radius $a = 45$ Å and charge $Q_{\text{core}} = n_{\text{core}} e_0 = +120 \ldots 220 e_0$ [31–33]. Extremely-basic H1

histones (existing in multiple subtypes [15]) are known to typically contain up to $Q_{\rm H1}=n_{\rm H1}e_0=+25\ldots55e_0$ charges [34, 35], depending on a number of conditions. H1 histones and their variants bind to the portion of linker DNA of length $L_{\rm link}$ which is not bound to the core. This (mostly ES) binding occurs at the positions where the DNA enters and exits the NCP [36–38]. Based on structural data, the NCP has rather a cylindrical shape, which is not very 'friendly' for exact computation of the ES energies. Furthermore, the exact geometry of individual NCPs becomes of secondary importance in large-scale toy models as depicted in figure 1. We thus base our mathematical model on a spherical easily-solvable NCP shape, bearing in mind that cylindrical geometry would just introduce slightly different numerical pre-factors, not affecting the major conclusions regarding NRL dependence on the amount of bound H1.

The total length of the histone-bound or immobilized DNA can then be written as

$$L_{\rm DNA}=NRL-L_{\rm link}. \tag{1}$$

The DNA length adsorbed in NCPs is $L=147\times3.4$ Å ≈500 Å for the canonical NCP structure [31]. We compute below the optimal DNA length L bound by the NCP with the total charge (core + H1)

$$Z([H1])=n_{core}+n_{H1}[H1]/[nuc]. \tag{2}$$

The latter depends on the stoichiometric ratio of the bound H1 per NCP, given in equilibrium by the ratio of their concentrations in the complex, [H1]/[nuc]. To evaluate NRL, we set the length of linker DNA to $L_{\rm link}=15$ bp. It might grow at higher [H1] due to steric effects imposed by bound H1 histones. Our ES-elastic model accounts for circular wrapping of the DNA around a spherical NCP core.

Using the Debye–Hückel potential of a sphere, the DNA-histone ES binding energy is [39]

$$E_{bind}\left(L_{DNA}\right)=-k_BT\left(Z-L_{DNA}/l_B\right)\times L_{DNA}e^{-\kappa(r-a)}/[r\,(1+\kappa a)] \tag{3}$$

Here, the DNA is neutralized according to the Manning's counterion condensation theory [40, 41]. This yields the effective DNA charge of about one e_0 charge per Bjerrum length $l_{\rm B}=e_0^2/(\varepsilon k_{\rm B}T)\approx7$ Å along the DNA axis. Here $k_{\rm B}T$ is the thermal energy, ε is the dielectric constant, and the radius of DNA-histone wrapping is $r=a+a_{\rm DNA}$ with $a_{\rm DNA}$ being the DNA radius. This means that DNA wrapping takes place directly on the histone sphere in our model. The reciprocal Debye screening length is κ that is $\kappa\approx1/(7$ Å) in a physiological solution with ≈0.1 M of 1:1 salt. In (3) the charge of already adsorbed DNA reduces the attraction caused by the histone core renormalizing the charge as $Z\text{->}(Z-L_{\rm DNA}/l_{\rm B})$. In our simplistic model we use the linear low-potential Debye–Hückel theory, valid for not too large histone charges and relatively high salt concentrations, such as e.g. $\kappa\approx1/(3$ Å) used in figure 2. The charge density used and somewhat elevated [electrolyte] guarantee the validity of the linear ES model.

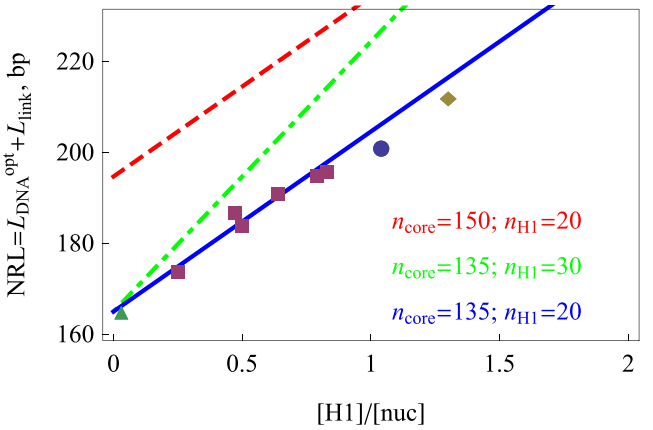

Figure 2. The variation of NRL with the amount of H1 bound to the histone core, plotted according to (6) for the three choices of n_{core} and n_{H1}, as indicated. In the model, the value of $L_{\rm DNA}$ at [H1] = 0 grows with the core histone charge n_{core}, while the slope of curves NRL([H1]) increases with linker histone charge n_{H1}. The value of $n_{H1}=20$ used for the solid blue curve is within the known range of H1 charge variation [34]. Parameters: $a=45$ Å, $a_{DNA}=9$ Å, $l_p=500$ Å, $l_B=7$ Å, $1/\kappa=3$ Å, $L_{link}=15bp$. The experimental points for NRLs are from [13]. The squares represent NRLs in the wild-type and H1-depleted mouse tissue cells [15] and embryonic stem cells [16], the diamond is the (H5 + H1)/NCP content of chicken erythrocyte chromatin [17], the circle is the data for glial nuclei from mammalian cerebral cortex [55], and the triangle is the NRL of Hho1-depleted yeast cells [56]. The solid line corresponds to the best fit ($n_{\rm core}$ = 135, $n_{\rm H1}$ = 20).

Also, the NCP crystal structures reveal that wrapped DNA contains plenty of mono- and divalent counterions in its grooves. For example [50] indicates a dozen of Mn^{2+} cations bound to the DNA: 20–50 mM of $MnCl_2$ is a prerequisite for successive NCP crystal formation buffers, affecting the cost of DNA bending [42]). How strongly the DNA charged state in NCPs differs from that in solution depends on a number of factors. This makes the study of counterion condensation onto NCP-associated DNA a separate non-trivial problem; some of its facets will be addressed in a longer study.

In the bound state, the Born ES self-energy of the histone sphere with the DNA of length $L_{\rm DNA}$ bound to it can be approximated as [39]

$$E_{self}\left(L_{DNA}\right)=k_BTl_B\left(Z-L_{DNA}/l_B\right)^2\Big/[2a\,(1+\kappa a)\,]. \tag{4}$$

Equation (4) assumes that the charges of bound DNA are effectively smeared over the histone sphere. This energy term is quadratic in $L_{\rm DNA}$ that enables us to compute the optimal length of the wrapped DNA. (4) shows that the more electroneutral NCP complexes become, the smaller the ES self-energy penalty gets, rendering DNA-histone complexation more stable. In the DNA unbound state we have $E_{\rm self}^0=E_{\rm self}(L_{\rm DNA}=0)$.

The elastic energy of a homogeneously bent double-stranded DNA around the core in the model of the worm-like chain is as follows

$$E_{bend}\left(L_{DNA}\right)=k_BTl_pL_{DNA}\Big/\Big[2r^2\Big]. \tag{5}$$

Here $l_{\rm p}=500\ldots750$ Å is the DNA persistence length including both mechanical and ES terms. The ES part of $l_{\rm p}$ is known

to be a sensitive function of the solution salinity, obeyed for the DNA as a quadratic law $l_p^{ES} \sim \kappa^{-2}$, see e.g. [43]. In our model, a non-fluctuating DNA fragment is strongly bound to the histone core, which is a valid approach for stiff polyelectrolytes such as DNA. We neglect sequence-specific effects both for DNA-histone binding and DNA elastic bending [44], ignoring also a possibility of energy-reducing kink deformations [45] and melting bubbles [46] in the DNA structure. Also, the ES penalty for DNA cyclization [47] is not included in the analysis. The implication of electric charges of the *free linker DNA* of potentially varying length onto NRL is neglected below as well.

In advanced ES models of NCP, one can account for a varying self-consistently determined radius of DNA wrapping r and also for ES interactions between the wrapped DNA fragments. The latter would alter the strength of DNA-histone attraction. Namely, stronger DNA-histone attraction would mimic the fact of ES DNA-DNA mutual attraction in NCPs. Strictly speaking, as the DNA is positioned close to the histone surface, negative image charges [48] will be created inside a low-dielectric hydrophobic histone core that in turn will repel the wrapped DNA. In addition, the DNA helical structure as well as the precise super-helical geometry of DNA wrapping will definitely affect the wrapping energetics. As we mentioned already, the DNA in NCPs often accumulates bound divalent cations in its grooves [49, 50] so the ES interactions between closely aligned DNA turns (DNA-DNA separation of ≈24 Å [31, 49]) can become attractive [51]. DNA helicity also non-trivially tunes the inter-nucleosomal interactions, turning them from repulsive to attractive at a close -range separation [52, 53]. All these complications are beyond the scope of this paper and will be treated elsewhere.

Results and discussion

From the energy of DNA-histone complex formation, $\Delta E(L_{\rm DNA}) = E_{\rm bind} + E_{\rm bend} + (E_{\rm self}\text{-}E^0_{\rm self})$, one can compute the optimal length of the histone-bound DNA $L_{\rm DNA}$ via the energy minimization as (in units of bp)

$$L_{DNA}^{opt}([H1]) = \frac{l_B}{3.4}\frac{\left[\begin{array}{c} Z([H1])\left(1 + ae^{-\kappa(r-a)}/r\right) \\ -l_p a(1+\kappa a)/\left(2r^2\right)\end{array}\right]}{1+2ae^{-\kappa(r-a)}/r}. \quad (6)$$

In the model, this DNA length is tightly bound by both the core and linker histones in NCPs. The sum of $L_{\rm DNA}$ from (6) and the linker DNA length, $NRL = L_{\rm DNA} + L_{\rm link}$, provides an estimate for NRL within this ES-elastic model. For realistic parameters used in figure 2, expression (6) provides a favorable agreement with the Woodcock *et al* experimental data [13] on the NRL growth with the amount of bound H1 histones per NCP.

Specifically, a realistic histone H1 charge of $n_{\rm H1}e_0 = 20e_0$ yields the correct slope for NRL([H1]) dependence. The slope of NRL increase is very sensitive to the amount of bound H1 per one NCP so that $n_{\rm H1} = 30$ yields already an incorrect NRL incline, the dot-dashed green curve in figure 2. Physically, as H1 concentration grows, longer DNA stretches are to be wrapped in NCP to maintain its electro-neutrality and ensure energetically-stable DNA-histone complex [54]. For the blue curve in figure 2, the best fit is achieved for the histone H1 charge of $+20e_0$. Upon addition of one H1 per NCP the amount of the NCP-associated DNA increases by about 40 bp, see figure 2. For the Manning-neutralized DNA used in our model, this corresponds to about $-20\ e_0$ charges on DNA, in complete agreement with the ES balance picture of H1 and DNA. DNA ES binding to the charges of core histone tunes the value $L_{\rm DNA}([{\rm H1}] = 0)$; in figure 2 the core histone charge is in a realistic range, $n_{\rm core}e_0 = 130\ldots150e_0$ [32].

Note that at salt concentrations used in figure 2, the linear Debye–Hückel ES theory can be applied, with the histone surface dimensionless ES potential being close to unity (∼25 mV). Also note that somewhat smaller $n_{\rm H1}$ and $n_{\rm core}$ in figure 2 from the experimentally measured histone charges can be reconciled if the condensation of counterions takes place not only onto DNA, but also onto histone proteins. We expect that the self-consistently determined fraction and distribution of condensed counterions on DNA and histone proteins upon their complexation has non-trivial implications on the NCP ES stability.

Subtracting the basal ES binding of DNA to the core histones, given by (3) with $Z = n_{\rm core}$, one can get the amplification factor for the change in the ES affinity due to bound H1 histones in the NCP, namely

$$\Delta K_{ES}\left(L_{DNA}\right) = \exp\left[\frac{L_{DNA}\, n_{H1}}{a\,(1+\kappa a)}\frac{[H1]}{[nuc]}\right]. \quad (7)$$

From this, the change in the dissociation constant ΔK_d can be computed between the state in the absence of bound H1 histones at $[{\rm H1}] = 0$ and the state with $[{\rm H1}]/[{\rm NCP}] = 1$. Namely, we get for the parameters of figure 2 that $\Delta K_d = 1M/\Delta K_{ES} \approx 10^{-6}M$.

As we mentioned above, H1-family proteins participate in architecturing chromatin-fiber structures. DNA stretches with very short linker DNA and almost no H1 are also capable of forming stable chromatin fibers, like those of yeast or neuronal cells. Note that the neuronal chromatin NRL data is not included in figure 2, due to an interplay of H1 and other NCP-associated proteins. Namely, MeCP2 proteins are extremely abundant in neuronal nuclei impacting the state of chromatin compaction [57]: they perform the role similar to that of H1 histones and have similarly located binding sites, but have different charge and geometry. The poly-dispersity of the DNA linker length severely affects the regularity of the chromatin fiber structures [58].

Conclusions and outlook

It is well-established that reduced contents of linker histones lead to a global reduction of spacing between nucleosomes in chromatin. In this study, we have exploited a simple

theoretical biologically-sound ES model describing the variation of NRL with the amount of H1 histones bound per NCP. We used realistic parameters for the histone core and H1 charges and accounted for charge screening in the system by a surrounding electrolyte. In our model, the addition of highly positively charged linker histones triggers ES binding of a proportionally longer stretch of DNA to the NCP, thereby leading to a longer total NRL. The increase is about 40 bp of NCP-associated DNA as a response to one NCP-bound H1 histone with 20 positive charges. It is in excellent agreement with the experimental data [13] and the charge stoichiometry of counterion-neutralized DNA and H1 histones. The current model offers a simple analytical rationale for NRL variation, which may be used i.e. in constructing large-scale 1D lattice models of gene regulation in a chromatin [12]. This important, but often under-appreciated, non-specific ES-balance mechanism of NRL regulation, apparently abundant in eukaryotic cells [59], is likely to interfere with strongly sequence-specific signals present in genomic DNA for regulating NCP positioning [3]. For the latter, anisotropic sequence-specific DNA bendability motifs are believed to prescribe the distinct positions for NCP binding on genomic DNAs.

Let us now briefly discuss the structure and role of linker histones and varying NRLs in chromatin organization. Histone H1 proteins feature positively charged terminal tails separated by a globular domain. The latter is believed to bind to the nucleosome, while the positively charged tails associate to and neutralize the charge of the linker DNA. H1 binding protects additional 15–20 bp of the linker nucleosomal DNA. Positively charged linker histones are known to regulate the chromatin compaction ability [1, 18], with H1-depleted chromatin having a tendency to de-condense [13, 15, 16]. Often, H1 linker histones induce a kind of attraction between neighboring NCPs yielding more compact and tightly wound structures. Bound H1 impose some geometrical restrictions on arrangements of the linker DNA, shaping thereby the structure of chromatin fibers. Similar to post-translational modifications of histone proteins and their tails, known to affect the higher order chromatin structure, the modifications of H1 charge do so as well. Linker histone phosphorylation, for example, has been suggested to play important roles in both chromatin condensation and transcriptional regulation. The level of reduction in H1-to-NCP stoichiometry leads to specific gene expression changes [15]. As we mentioned in the introduction, strong correlations exist of NRL decrease upon reduction of the concentration of bound H1 per NCP, or for smaller positive H1 charges [13]. Depletion of H1 proteins associated with the chromatin fibers inevitably leads to a reduction of NRL. This ES mechanism provides a simple and non-specific rationale to regulate NRL and the degree of compaction of chromatin fibers in eukaryotes. The prerequisite to satisfy the ES balance is a shortening of the DNA length as the positive charge or amount of NCP-bound H1/H5 proteins is reduced.

With the exception of budding yeast which has a very short NRL and low H1/NCP ratio, the majority of cells and organisms have between 0.5 and 1 H1 proteins associated per NCP [13] (with the canonical value being H1/NCP ~ 1). The H1/NCP content is likely to vary with the degree of compaction of chromatin fibers, likely being inhomogeneous along the structure. This might lead to some experimental artefacts when computing the average content per NCP for the entire fiber, see for example the discussion in [55]. Although the abundances of H1-subtype histone proteins are delicately regulated in cells, the global reduction of NRL is possible if the up-regulation cellular mechanisms are forced beyond their limits. Other compensatory mechanisms of ES H1-NCP imbalance can be at work such as strongly DNA binding proteins and polyamines. Other non-histone proteins can compete for the linker DNA stretches and, if being positively charged, restore the ES balance of H1/NCP in chromatin. This opens new perspectives for future theoretical studies.

Acknowledgements

ACG acknowledges funding from the Deutsche Forschungsgemeinschaft (DFG Grant CH 707/5-1). VBT acknowledges support by the Heidelberg Center for Modeling and Simulation in the Biosciences (BIOMS) and a DKFZ Intramural Grant.

References

[1] Wolffe A 1998 *Chromatin: Structure and Function* (San Diego: Academic Press) p 447
[2] Schiessel H 2003 The physics of chromatin *J. Phys.: Cond. Matt.* **15** R699–R774
[3] Segal E *et al* 2006 A genomic code for nucleosome positioning *Nature* **442** 772–8
[4] Teif V B *et al* 2012 Genome-wide nucleosome positioning during embryonic stem cell development *Nature Struct. Mol. Biol.* **19** 1185–92
[5] Mobius W *et al* 2013 Toward a unified physical model of nucleosome patterns flanking transcription start sites *Proc. Natl. Acad. Sci. USA* **110** 5719–24
[6] Teif V B and Rippe K 2012 Calculating transcription factor binding maps for chromatin *Brief. Bioinform.* **13** 187–201
[7] Mirny L A 2010 Nucleosome-mediated cooperativity between transcription factors *Proc. Natl. Acad. Sci. USA* **107** 22534–9
[8] Teif V B *et al* 2013 Taking into account nucleosomes for predicting gene expression *Methods* **62** 26–38
[9] Teif V B and Rippe K 2011 Nucleosome mediated crosstalk between transcription factors at eukaryotic enhancers *Phys. Biol.* **8** 044001
[10] Li G, Levitus M, Bustamante C and Widom J 2005 Rapid spontaneous accessibility of nucleosomal DNA *Nature Struct. Mol. Biol.* **12** 46–53
[11] Teif V B and Rippe K 2010 Statistical-mechanical lattice models for protein-DNA binding in chromatin *J. Phys.: Cond. Matt.* **22** 414105
[12] Beshnova D A, Cherstvy A G, Vainshtein Y and Teif V B 2014 Regulation of the nucleosome repeat length in vivo by the DNA sequence, protein concentrations and long-range interactions *PLoS Comp. Biol.* **10** e1003698
[13] Woodcock C L, Skoultchi A I and Fan Y 2006 Role of linker histone in chromatin structure and function: H1

stoichiometry and nucleosome repeat length *Chromos. Res.* **14** 17–25
[14] Blank T A and Becker P B 1995 Electrostatic mechanism of nucleosome spacing *J. Mol. Biol.* **252** 305–13
[15] Fan Y *et al* 2003 H1 linker histones are essential for mouse development and affect nucleosome spacing in vivo *Mol. Cell. Biol.* **23** 4559–72
[16] Fan Y *et al* 2005 Histone H1 depletion in mammals alters global chromatin structure but causes specific changes in gene regulation *Cell* **123** 1199–212
[17] Bates D L and Thomas J O 1981 Histones H1 and H5: one or two molecules per nucleosome? *Nucl. Acids Res.* **25** 5883–94
[18] Clark D J and Kimura T 1990 Electrostatic mechanism of chromatin folding *J. Mol. Biol.* **211** 883–96
[19] Harshman S W *et al* 2013 H1 histones: current perspectives and challenges *Nucl. Acids Res.* **41** 9593–609
[20] Trifonov E N and Sussman J L 1980 The pitch of chromatin DNA is reflected in its nucleotide sequence *Proc. Natl. Acad. Sci. USA* **77** 3816–20
[21] Potoyan D A and Papoian G A 2012 Regulation of the H4 tail binding and folding landscapes via Lys-16 acetylation *Proc. Natl. Acad. Sci. USA* **109** 17857–62
[22] Boroudjerdi H, Naji A and Netz R R 2014 Global analysis of the ground-state wrapping conformation of a charged polymer on an oppositely charged nano-sphere *Europ. Phys. J.* E **37** 21
[23] Kim W K and Sung W 2013 How charge fluctuations modulate complexation of DNA around a histone cylinder *Europhys. Lett.* **104** 18002
[24] Boroudjerdi H, Naji A and Netz R R 2011 Salt-modulated structure of polyelectrolyte-macroion complex fibers *Europ. Phys. J.* E **34** 72
[25] Messina R 2009 Electrostatics in soft matter *J. Phys.: Cond. Matt.* **21** 113102
[26] Ulrich S, Seijo M and Stoll S 2006 The many facets of polyelectrolytes and oppositely charged macroions complex formation *Curr. Opin. Coll. Interf. Sci.* **11** 268–72
[27] Cao Q and Bachmann M 2013 Polyelectrolyte adsorption on an oppositely charged spherical polyelectrolyte brush *Soft Matter* **9** 5087–98
[28] Depken M and Schiessel H 2009 Nucleosome shape dictates chromatin fiber structure *Biophys. J.* **96** 777–84
[29] Robinson P J J, Fairall L, Huynh V A T and Rhodes D 2006 EM measurements define the dimensions of the '30 nm' chromatin fiber: Evidence for a compact, interdigitated structure *Proc. Natl. Acad. Sci. USA* **103** 6506–11
[30] Routh A, Sandin S and Rhodes D 2008 Nucleosome repeat length and linker histone stoichiometry determine chromatin fiber structure *Proc. Natl. Acad. Sci. USA* **105** 8872–7
[31] Luger K, Maeder A W, Richmond R K, Sargent D F and Richmond T J 1997 Crystal structure of the nucleosome core particle at 2.8 Å resolution *Nature* **389** 251–60
[32] Cherstvy A G 2009 Positively charged residues in DNA-Binding domains of structural proteins follow sequence-specific positions of DNA phosphate groups *J. Phys. Chem.* B **113** 4242–7
[33] Fenley A T, Adams D A and Onufriev A V 2010 Charge state of the globular histone core controls stability of the nucleosome *Biophys. J.* **99** 1577–85
[34] Subirana J A 1990 Analysis of the charge distribution in the C-terminal region of histone H1 as related to its interaction with DNA *Biopolymers* **29** 1351–7
[35] Dootz R, Toma A C and Pfohl T 2011 Structural and dynamic properties of linker histone H1 binding to DNA *Biomicrofluid.* **5** 024104
[36] Syed S H *et al* 2010 Single-base resolution mapping of H1-nucleosome interactions and 3D organization of the nucleosome *Proc. Natl. Acad. Sci. USA* **107** 9620–5
[37] Pachov G V, Gabdoulline R R and Wade R C 2011 On the structure and dynamics of the complex of the nucleosome and the linker histone *Nucl. Acids Res.* **39** 5255–63
[38] Zhou B R *et al* 2013 Structural insights into the histone H1-nucleosome complex *Proc. Natl. Acad. Sci. USA* **110** 19390–5
[39] Cherstvy A G and Winkler R G 2005 Simple model for overcharging of a sphere by a wrapped oppositely charged asymmetrically neutralized polyelectrolyte: possible effects of helical charge distribution *J. Phys. Chem.* B **109** 2962–9
[40] Manning G S 1978 The molecular theory of polyelectrolyte solutions with applications to the electrostatic properties of polynucleotides *Quart. Rev. Biophys.* **11** 179–246
[41] Manning G S 2001 Counterion Condensation on a Helical Charge Lattice *Macromol.* **34** 4650–5
[42] Podgornik R 2006 DNA off the Hooke *Nature Nanotech.* **1** 100–1
[43] Savelyev A, Materese C K and Papoian G A 2011 Is DNA's rigidity dominated by electrostatic or non-electrostatic interactions? *J. Am. Chem. Soc.* **133** 19290–3
[44] Peters J P *et al* 2013 Mechanical properties of DNA-like polymers *Nucl. Acids Res.* **41** 10593–604
[45] Vologodskii A and Frank-Kamenetskii M D 2013 Strong bending of the DNA double helix *Nucl. Acids Res.* **41** 6785–92
[46] Shin J, Cherstvy A G and Metzler R 2014 Sensing Viruses by Mechanical Tension of DNA in Responsive Hydrogels *Phys. Rev.* X **4** 021002
[47] Cherstvy A G 2011 DNA cyclization: suppression or enhancement by electrostatic repulsions? *J. Phys. Chem.* B **115** 4286–94
[48] Cherstvy A G 2007 Effect of a low-dielectric interior on DNA electrostatic response to twisting and bending *J. Phys. Chem.* B **111** 12933–7
[49] Tan S and Davey C A 2011 Nucleosome structural studies *Curr. Opin. Struct. Biol.* **21** 128–36
[50] Wu B and Davey C A 2010 Using soft x-rays for a detailed picture of divalent metal binding in the nucleosome *J. Mol. Biol.* **398** 633–40
[51] Cherstvy A G 2009 Probing DNA-DNA electrostatic friction in tight superhelical DNA plies *J. Phys. Chem.* B **113** 5350–5
[52] Cherstvy A G and Everaers R 2006 Layering, bundling, and azimuthal orientations in dense phases of nucleosome core particles *J. Physics: Cond. Matt.* **18** 11429–42
[53] Cherstvy A G and Teif V B 2013 Structure-driven homology pairing of chromatin fibers: the role of electrostatics and protein-induced bridging *J. Biol. Phys.* **39** 363–85
[54] Winkler R G and Cherstvy A G 2014 Strong and weak polyelectrolyte adsorption onto oppositely charged curved surfaces *Adv. Polym. Sci.* **255** 1–56
[55] Pearson E C, Bates D L, Prospero T D and Thomas J O 1984 Neuronal nuclei and glial nuclei from mammalian cerebral cortex Nucleosome repeat lengths, DNA contents and H1 contents *Eur. J. Biochem.* **144** 353–60
[56] Freidkin I and Katcoff D J 2001 Specific distribution of the Saccharomyces cerevisiae linker histone homolog HHO1p in the chromatin *Nucl. Acids Res.* **29** 4043–51
[57] Skene P J *et al* 2010 Neuronal MeCP2 is expressed at near histone-octamer levels and globally alters the chromatin state *Mol. Cell* **37** 457–68
[58] Collepardo-Guevara R and Schlick T 2014 Chromatin fiber polymorphism triggered by variations of DNA linker lengths *Proc. Natl. Acad. Sci. USA* PNAS Early Edition
[59] Korolev N, Allahverdi A, Lyubartsev A P and Nordenskiöld L 2012 The polyelectrolyte properties of chromatin *Soft Matter* **8** 9322–33